ROYAL SOCIETY OF CHEMISTRY

PAPER

Check for updates

Estimating NH₃ and PM₂.₅ emissions from the Australia mega wildfires and the impact of plume transport on air quality in Australia and New Zealand

Ece Ari Akdemir, William H. Battye, Casey Bray Myers [iD] * and Viney P. Aneja

Due to the highly flammable biota and a shortfall of precipitation in Australia, wildfires (bushfires) are connected with Australia's ecology and culture. These wildfires affect air quality, emitting ammonia (NH₃) and fine particulate matter (PM₂.₅), among other pollutants, into the atmosphere. Record breaking temperatures and drought contributed to the unprecedented 2019–2020 Australian wildfire season in Southeastern Australia. The objective of this study is to calculate emissions of $PM_{2.5}$ and NH_3 from wildfires from December 29, 2019, to January 4, 2020 and to analyze the air quality impact on Southeast Australia associated with these mega wildfires. Emissions of $PM_{2.5}$ and NH_3 were calculated using a combination of satellite data for burn area and land classification and emissions factors from the literature. The impact of $PM_{2.5}$ in Southeast Australia, Southwest shore of New Zealand, and the inner part of Australia were estimated by performing a Hybrid Single-Particle Lagrangian Integrated Trajectory (HYSPLIT) analysis. The results of this work show that fire activity in the study region produced 526 569 125 kg of NH_3 and 41 167 586 kg of $PM_{2.5}$ during the period of interest. Between December 29, 2019, and January 4, 2020, hourly concentrations of $PM_{2.5}$ reached 2496.1 $\mu g\ m^{-3}$ in Australia and 48.8 $\mu g\ m^{-3}$ in New Zealand, exceeding the national standard of 25 $\mu g\ m^{-3}$ a total of 100 and 2 times, respectively, which suggests the influence the fires have on air quality in the region.

Environmental significance

Wildfire activity is significant in Australia due to the highly flammable biota. These wildfires emit mass amounts of pollutants into the atmosphere, thus negatively impacting air quality. This study analyzes the impact that emissions of ammonia and fine particulate matter from wildfires have on air quality in Southeast Australia and Southwest New Zealand during 2019/2020. Exposure to elevated concentrations of these pollutants is associated with a variety of health impacts ranging from increased asthma to death.

1. Introduction

Wildfires are described as uncontrollable and unforeseen fires.[1] Mega wildfires (whose characteristics include duration, high intensity and fast rates of spread) are responsible for significant human, environmental, economic, and ecological impacts. In Australia's history, wildfires (bushfires) are directly connected with Australia's ecology and culture.[2] Australia has more fire-prone lands than the other continents due to the highly flammable biota.[3] In Victoria state, bushfires have produced damage worth $2.5 billion and caused approximately 300 deaths with many injuries in the past century.[4,5] While the primary impact of bushfires is damaging property, they also emit a significant quantity of pollutants into the atmosphere thus negatively impacting air quality on a local and regional scale.[6–12]

During biomass burning, various gaseous and aerosols are emitted into the atmosphere, including sulfur dioxide (SO_2), carbon monoxide (CO), carbon dioxide (CO_2), volatile and semi-volatile organic compounds (VOC & SVOC), methane (CH_4), ammonia (NH_3), and particulate matter.[12–14] Exposure to elevated concentrations of $PM_{2.5}$ has a negative impact on both human health and the environment.[15,16] For example, a recent study by Aguilera *et al.* (2021) on the health impact of wildfire smoke in Southern California suggests that recent animal toxicological studies suggest that particulate matter from wildfires is potentially more toxic than equal doses from other sources such as ambient pollution.[17] In addition to the impact on human health, $PM_{2.5}$ also reduces visibility. Reducing visibility has become an important problem in various environments such as wilderness areas and national parks.[15,18]

Department of Marine, Earth, and Atmospheric Sciences, North Carolina State University, Raleigh, NC, 27695, USA. E-mail: cdbray@ncsu.edu

Emissions of NH_3 play a critical role in the formation of secondary fine particulate matter.[19–26] In addition to contributing to the formation of secondary $PM_{2.5}$, elevated emissions of NH_3 can also lead to ammonification, eutrophication, loss of biodiversity and a decreased resistance to drought and frost damage.[25,27] NH_3 can also play a role in the formation of nitrous oxide (N_2O), which is a greenhouse gas with a warming potential that is nearly 300 times that of carbon dioxide (CO_2).[11]

The changing climate has had a significant impact on wildfire activity, at a global and regional scale, over the past few decades.[14,28] Fire conditions are triggered by dry, windy, and hot ambient conditions.[3] Moreover, as the climate warms and dries, the decomposition slows and litter fuel accumulates faster enhancing fire intensity and fast rate of fire spread.[29] With the record-breaking temperatures in the 2019–2020 summer season, bushfires ramped up significantly after the drought season.[30,31] This resulted in an unprecedentedly devastating 2019/2020 Australian fire season, with hundreds of fires and more than 23% of the temperate forests burned.[28] These fires had a significant impact on air quality across the region. For example, Shiraishi and Hirata (2021) quantified emissions of CO_2 from these fires and found that the emissions in December 2019 were the highest on record since 2001 and they represented 64% of the Australian average annual emissions from 2001–2018.[32] Similarly, Li *et al.* (2021) quantified emissions of CO_2 from November 2019 to January 2020 and found that the

emissions accounted for 35% of Australia's greenhouse gas emissions from all sectors in 2020.[33] Graham *et al.* (2021) estimated the impact these fires had on Eastern Australia using WRF-Chem and found that the average observed $PM_{2.5}$ concentrations were over 3 times higher than concentrations modeled without fires. Graham *et al.* (2021) found that the elevated concentrations of $PM_{2.5}$ exposed an additional ~437 000 people to Air Quality Index (AQI) values in the 'Poor', 'V. Poor' and 'Hazardous' range.[34]

Due to the significance of the 2019/2020 fire season, the objective of this study is to quantify emissions of NH_3 and $PM_{2.5}$ from Australia's mega wildfires in Southeast Australia, which peaked from December 29, 2019, to January 4, 2020, and analyze their impact on local and regional air quality. Emissions were quantified using a combination of satellite data and emission factors. Due to the nature of emission inventory creation, there is significant variability between different parameters used to estimate emissions (*e.g.* emissions factors, land classification). Because of this, emissions from these mega wildfires were calculated using a range of emissions factors and a sensitivity analyses was performed. The Hybrid Single-Particle Lagrangian Integrated Trajectory (HYSPLIT)[35] model and ambient air quality data were used to determine the impact of these emissions had on air quality in Southeast Australia and New Zealand.

2. Data and methodology

NH_3 and $PM_{2.5}$ emissions from wildfires were calculated using eqn (1):[11,13,36,37]

$$E_i = B(x) \times BA(x,t) \times EF_j \times FB, \tag{1}$$

where E_i represents the species' emissions (g), $B(x)$ represents the biomass loading, which is the amount of biomass available to be burned based on land cover type, at location x (g m^{-2}), $BA(x,t)$ represents the burned area at location x and time t (m^2), EF_j represents the emission factor for species j (g species per g

Table 1 Summary of methodology used to estimate the fraction of biomass burned (FB) based on the work of Ito and Penner (2004) and Wiedinmyer *et al.* (2006, 2011).[13,37,40] Table was adapted from Bray *et al.* (2021).[14] Percent of tree cover was assumed based on land classification dataset description

Tree cover	Woody fuel	Herbaceous fuel
60%+	0.3	0.9
40–60%	0.3	$e^{-0.13 \times \text{Fraction Tree Cover}}$
<40%	0	0.98

Table 2 Biomass loading (g m^{-2}), the fraction of biomass, and the emission factor of NH_3 and $PM_{2.5}$ (g species per g biomass burned) for each land cover type

Name	Biomass loading (g m^{-2})	Fraction of biomass	Emission factor (g species per g biomass burned)	
			PM$_{2.5}$	NH$_3$
Evergreen needleleaf forests	11 696[a]	0.3	0.0121[b]	0.0009[b]
Evergreen broadleaf forests	11 696[a]	0.3	0.0099[b]	0.0007[b]
Deciduous broadleaf forests	11 696[a]	0.3	0.0099[b]	0.0007[b]
Mixed forests	11 696[a]	0.3	0.0099[b]	0.0007[b]
Open forests	11 696[a]	0.3	0.0121[b]	0.0009[b]
Sparse forests	11 696[a]	0.98	0.0121[b]	0.0009[b]
Dense herbaceous	245[a]	0.98	0.0056[b]	0.0006[b]
Sparse herbaceous	245[a]	0.96	0.0056[b]	0.0006[b]
Dense shrublands	1271[a]	0.30	0.0057[b]	0.0015[b]
Shrubland/grassland mosaics	1271[a]	0.96	0.0095[b]	0.0006[b]
Sparse shrublands	1271[a]	0.96	0.0057[b]	0.0015[b]

[a] Ref. 37. [b] Ref. 13.

© 2022 The Author(s). Published by the Royal Society of Chemistry

Environ. Sci.: Atmos., 2022, **2**, 634–646 | **635**

Table 3 Highest and lowest emission factors for $PM_{2.5}$ and NH_3 used in sensitivity analysis

| Name | Emission factor (g species per g biomass burned) | | | |
| | $PM_{2.5}$ | | NH_3 | |
	Highest factor	Lowest factor	Highest factor	Lowest factor
Evergreen needleleaf forests	0.033[a]	0.004[a]	0.0017[a]	0.00029[c]
Evergreen broadleaf forests	0.013[a]	0.005[c]	0.0025[a]	0.00012[a]
Deciduous broadleaf forests	0.013[b]	0.005[c]	0.0025[a]	0.00012[a]
Mixed forests	0.013[b]	0.005[c]	0.0025[a]	0.00012[a]
Open forests	0.033[a]	0.004[a]	0.0017[a]	0.00029[c]
Sparse forests	0.033[a]	0.004[a]	0.0017[a]	0.00029[c]
Dense herbaceous	0.013[a]	0.004[a]	0.0016[a]	0.00036[a]
Sparse herbaceous	0.013[a]	0.004[a]	0.0016[a]	0.00036[a]
Dense shrublands	0.011[b]	0.004[a]	0.0009[a]	0.00017[a]
Shrubland/grassland mosaics	0.018[b]	0.004[a]	0.0017[c]	0.00037[a]
Sparse shrublands	0.011[b]	0.004[a]	0.0009[a]	0.00017[a]

[a] Ref. 42. [b] Ref. 43. [c] Ref. 44.

biomass burned) and FB represents the fraction of biomass burned. The biomass loading (B) values, which are region specific, were obtained from Wiedinmyer et al. (2011) and are presented in Table 2.[37] Land cover classification was identified using the Collection 5 MODIS Global Land Cover Type product (MCD12Q1; 500 m) Version 6 for 2018.[38] Because these fires occurred in Southeastern Australia, all tree land classifications were assumed to be temperate. Burn area (BA) was determined using the Collection 6 of the Moderate Resolution Imaging Spectroradiometer (MODIS)/Aqua + Terra Thermal Anomalies/Fire locations near-real-time (NRT) product (MCD14DL; 1 km). This product is processed by NASA's LANCE (Land, Atmosphere Near real-time Capability for EOS) Fire Information for Resource Management System (FIRMS), using swath products (MOD14/MYD14).[39] The fraction of biomass burned (FB) was determined based on tree coverage percent following the work of Wiedinmyer et al. (2006) and Wiedinmyer et al. (2011), which was adapted from Ito and Penner (2004).[13,37,40] This methodology is summarized in Table 1.[14] The assumed fraction of biomass burned are available in Table 2 and are based on the land classification dataset (MCD12Q1). Average emission factors (EF) for $PM_{2.5}$ and NH_3 were obtained from the literature[13,37] and are represented in Table 2.

Because emission factors can vary significantly between inventories, a sensitivity analysis was also conducted using a range of emission factors from the Smoke Emissions
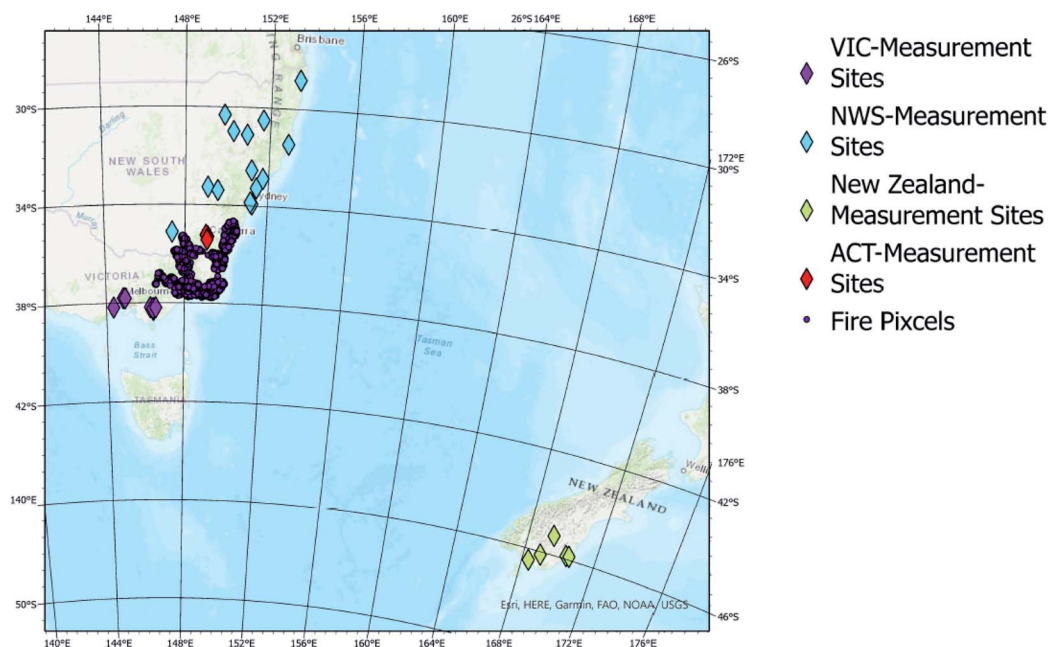

Fig. 1 Location of the measurement sites in relation to the fire pixels.

Table 4   Measurement sites associated with organization

Organization	Site name
ACT	Florey
ACT	Monash
NSW	Lismore
NSW	Wagga Wagga North
NSW	Orange
NSW	Bathurst
NSW	Randwick
NSW	Rozelle
NSW	Wyong
NSW	Mayfield
NSW	Singleton South
NSW	Narrabri
NSW	Gunnedah
NSW	Tamworth
NSW	Armidale
NSW	Port Macquarie
VIC	Footscray
VIC	Melbourne
VIC	Churchill
VIC	Moe
New Zealand	Dunedin
New Zealand	Mosgiel
New Zealand	Alexandra at 5 Ventry street
New Zealand	Invercargill at Pomona street
New Zealand	Gore at Main street

Reference Application (SERA), which are obtained from the literature.[41] Table 3 shows the highest and lowest emission factors from SERA that are used to compare against the average emission factors described in Table 2. Estimated emissions using the highest, lowest, and average emission factors were compared against FINN (Fire Inventory from the National Center for Atmospheric Research (NCAR)), version 2.4, using the MODIS only input. In addition to this, estimated emissions of $PM_{2.5}$ using the highest, lowest and average emission factors were used in the HYSPLIT model to compare against the observed concentrations of $PM_{2.5}$ during the study period.

Ground based monitoring sites located in the study region were used to determine the impact the fires had on $PM_{2.5}$

Table 5   Burned areas in Australia (km^2) and emissions of $PM_{2.5}$ and NH_3 (kg) from December 29, 2019, to January 4, 2020

Land classification	Burned area (km^2)	$PM_{2.5}$ (kg)	NH_3 (kg)
Evergreen needleleaf forests	4090	177 677 585	13 614 658
Evergreen broadleaf forests	5732	199 910 614	16 868 380
Deciduous broadleaf forests	23	863 409	72 143
Mixed forests	519	18 923 362	1 381 474
Open forests	1413	61 930 940	4 631 183
Sparse forests	401	58 426 488	3 869 023
Dense herbaceous	1903	7 772 237	644 068
Sparse herbaceous	1.3	1698	182
Dense shrublands	40	37 303	21 386
Shrubland/grassland mosaics	92	1 025 132	64 995
Sparse shrublands	0.1	356	94
Total	14 230	526 569 125	41 167 586

concentrations (Fig. 1). These monitoring sites operate under the Planning, Industry and Environment unit of the New South Wales Government (NSW; 14 monitors), the Australian Capital Territory (ACT; 2 monitors), the Environmental Protection Authority Victoria (VIC; 4 monitors), and the Ministry for the Environment of New Zealand (New Zealand; 5 monitors). Table 4 lists the measurement sites associated with each organization. While the monitoring sites in Australia are impacted by urban and rural activities (*e.g.*, traffic and agriculture), the monitoring sites in New Zealand are located in remote locations with low population density.[45] Hourly $PM_{2.5}$ concentrations were measured using Thermo FH62C14 continuous ambient particulate monitors with a minimum detection limit of 4 μg m^{-3}.[46] These data have undergone preliminary quality analysis. To be consistent with the detection limit, each measurement lower than the detection limit is set as the same as the detection limit. While a number of measurement sites were examined in this work, only a select few will be examined in the manuscript.

The HYSPLIT model (1 km),[35,47] with meteorological data from the National Center for Environmental Prediction (NCEP) NCAR Global Reanalysis Data Archive (2.5°) and emissions data calculated in this study, was run every 12 hours with a 48 h forward trajectory at 500 m from December 29, 2019, to January 4, 2020, to examine the impact the Australian mega wildfires had on ambient concentrations of $PM_{2.5}$ and NH_3. The HYSPLIT model provided both trajectory and pollutant concentrations at 1 km horizontal resolution. For comparison, the model was also run using emissions from FINNv2.4.

3.   Results

Between December 29, 2019, and January 4, 2020, forest fires in the study region consumed 14 230 km^2 of land, with evergreen needleleaf and broadleaf forests being the most heavily impacted (Table 5). These fires produced 526 569 125 kg of NH_3 and 41 167 586 kg of $PM_{2.5}$ during the study period. The lowest burned area was observed on December 29, 2019 (493 km^2) while the highest burned area was observed on January 4, 2020 (5 286 587 330 km^2). Fig. 2 shows the total daily emissions of both $PM_{2.5}$ and NH_3. Emissions of $PM_{2.5}$ from the forest fires in the study region ranged from 17 338 953 kg (December 29, 2019) to 200 481 575 kg (January 4, 2020), with a total of 526 569 125 kg emitted during the study period. Similarly, emissions of NH_3 ranged from 919 622 kg (January 1, 2020) to 14 570 058 kg (January 4, 2020). Because burn area is the dominating parameter in emission calculations, it is not surprising that the general trend of the species emissions follows the trend of area burned with the maximum emissions occurring on the day with the maximum area burned. However, the minimum emissions of $PM_{2.5}$ and NH_3 occurred on different days which can likely be attributed to the location of the areas burned and the associated emission factors.

In addition to calculating emissions using the average emission factors in the literature, a sensitivity analysis was performed using the highest and lowest end of emission factors in the literature (Fig. 3). As expected, emissions were highest using the highest emissions factor, ranging from 26 163 241 kg
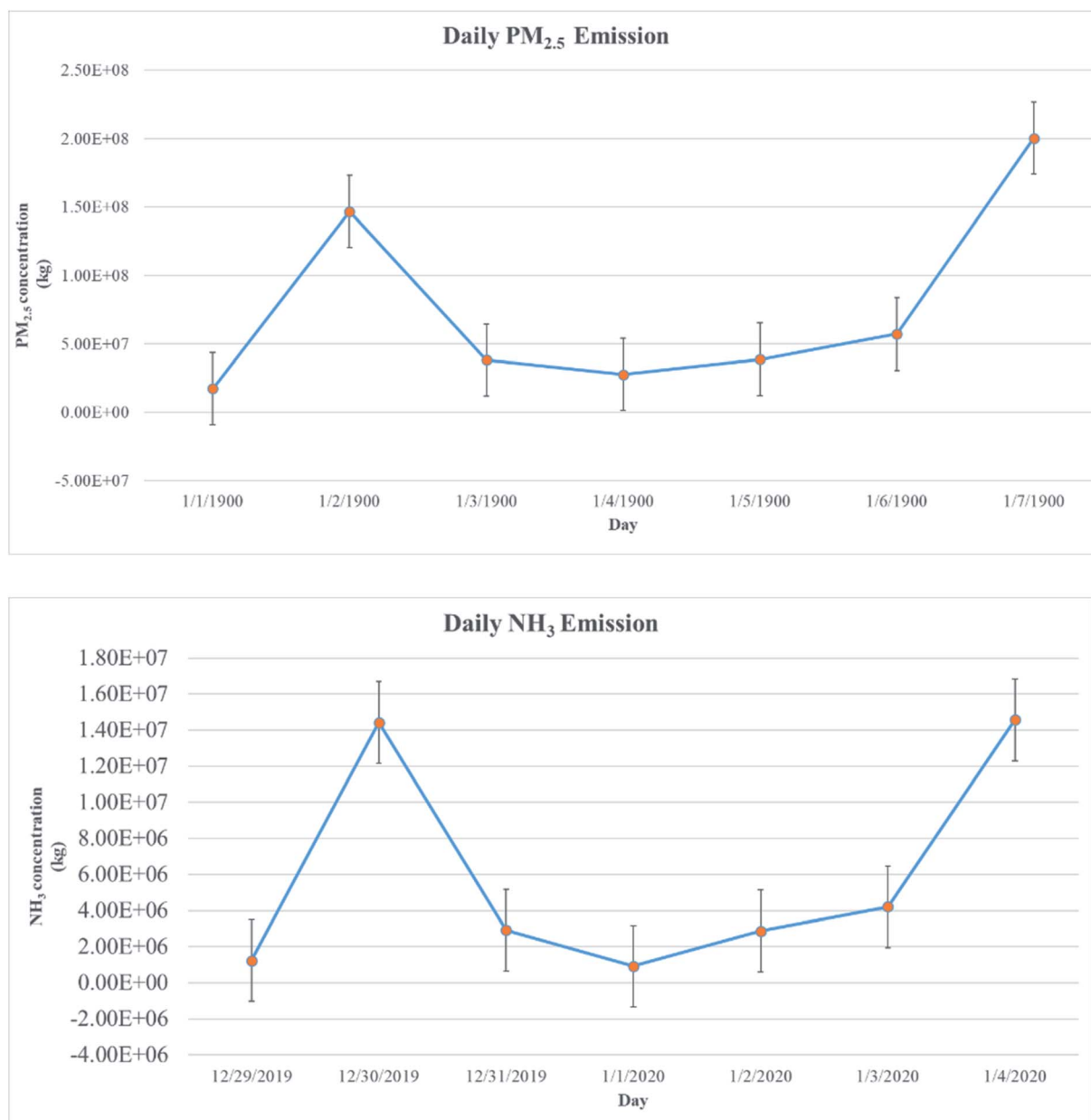
© 2022 The Author(s). Published by the Royal Society of Chemistry

Environ. Sci.: Atmos., 2022, **2**, 634–646 | **637**

Fig. 2 Daily $PM_{2.5}$ emissions and NH_3 emissions in Southeast Australia during the study period. The circles represent burned area, $PM_{2.5}$ and NH_3 emissions as m^2 per day and billions g per day, respectively. The gray lines represent the changes between days. Black vertical bars in the figure represent ± 1 SD.

to 405 878 823 kg for $PM_{2.5}$ and ranging from 1 978 897 kg to 39 119 703 kg for NH_3. Similarly, emissions were lowest using the lowest emission factor, ranging from 8 289 600 kg to 84 025 943 kg for $PM_{2.5}$ and ranging from 244 209 kg to 3 682 299 kg.

The calculated emissions from biomass burning were also compared with FINN version 2.4 with the MODIS fire inputs (Fig. 3). The results of this comparison show that the FINN estimates are comparable to the estimates, with the FINN estimates generally falling between the emissions calculated created the highest and emission factors. FINN emission estimates of $PM_{2.5}$ were on average, 70% higher than emissions

calculated with the average emission factor, ranging from 22% lower on December 29, 2019, to 192% higher on December 31, 2021. FINN estimates were consistently higher than the NH_3 emissions estimated created using the average emissions factor in this work ranging from 47% (December 30, 2019) higher to 993% higher (January 2, 2019), with the emissions estimated in this work being, on average, 264% lower. FINN estimates were closest to emission estimates created using the highest emission factor, with the estimated emissions an average of 17% higher and 78% lower than the FINN emissions for $PM_{2.5}$ and NH_3, respectively. When comparing the $PM_{2.5}$ emissions calculated using the highest emissions factor, FINN estimated
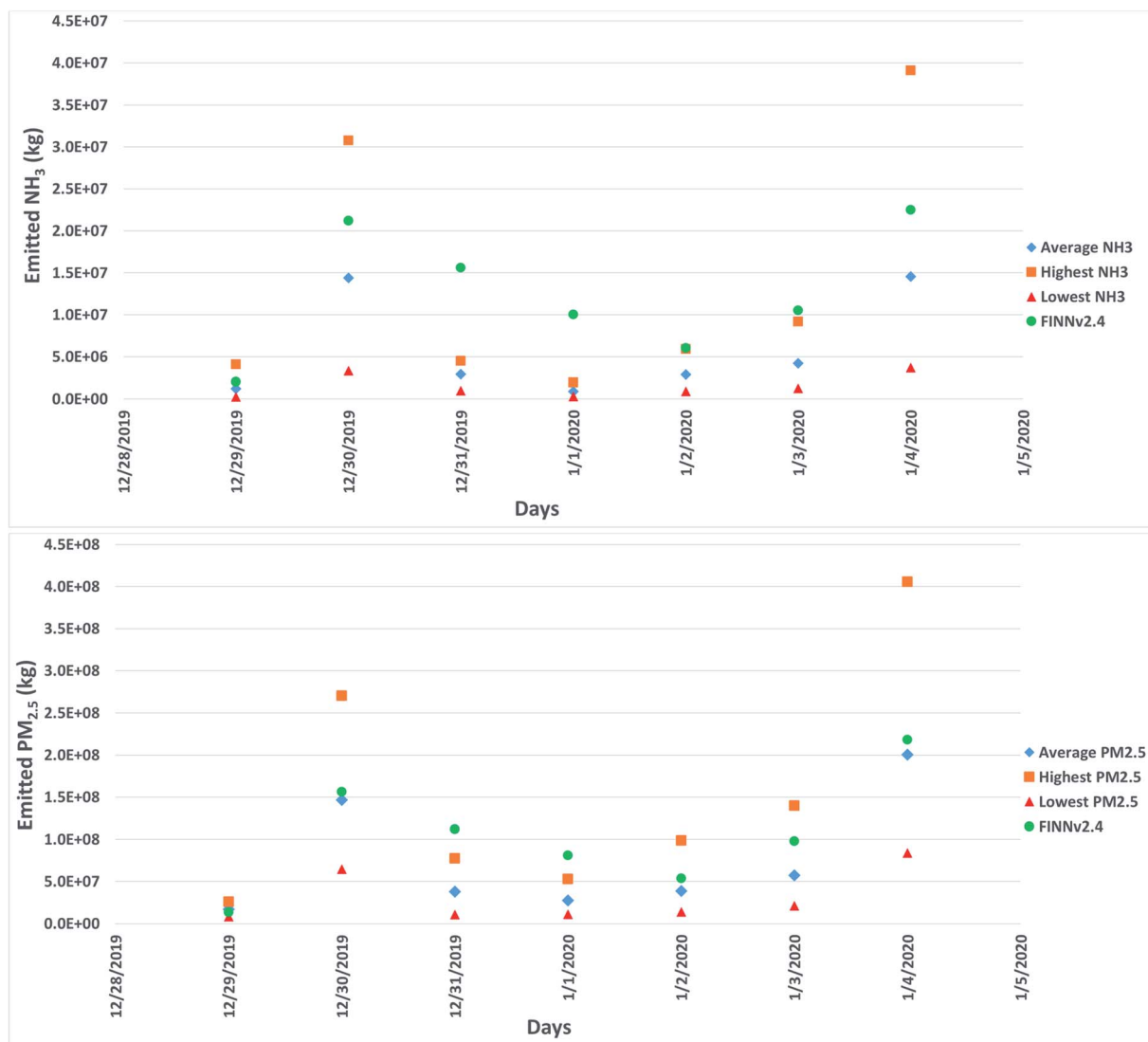
Fig. 3   Daily total emissions of NH_3, and $PM_{2.5}$ from biomass burning during the timeline, calculated using both the average emission factors and the highest and lowest end of emission factors from the literature.

emissions ranged from 53% higher on January 1, 2020, to 42% lower than the emissions estimated in this study on December 30, 2019. Similarly, the NH_3 emissions estimated using the highest factor ranged from 51% higher (December 29, 2019) to 408% lower (January 1, 2020) than the NH_3 emissions estimated by FINN. The emission estimates in this study using the lowest emission factor were consistently lower than the emission estimates, ranging from 63% lower (December 29, 2019) to 948% (December 31, 2019) for $PM_{2.5}$ and 511% (January 4, 2020) to 3218% (January 1, 2020) lower for NH_3.

Due to the nature of emission inventories, the differences between FINNv2.4 and this work was expected. Similar differences were observed by Li *et al.* (2021), who compared quantified emissions of CO_2 from the Australian mega fires from November 2019 to January 2020 with FINNv1.5, FINNv2.4, Shiraishi and Hirata (2021) and the Global Fire Assimilation System (GFASv1.2).[32,33] Li *et al.* (2021) attributed these

differences to differences in the estimation techniques used as well as differences in the parameters used to create the emissions.[33] The differences between FINN and the estimated emissions in this study can be attributed to the different inputs used in the emission estimation equation. While this work follows the methodology of Wiedinmyer *et al.* (2006) and (2011), because the inputs were different, the emission estimates were different.[13,37] Burn area calculated in this study was also compared with the burn area calculated by FINNv2.4 (Fig. 4). The burn area calculated in this study was on average 42% lower than the burn area calculated in FINN. The largest difference in burn areas were observed on December 31, 2019, and January 1, 2020, with the burn area used in this work 153% and 91% lower than the burn area in FINN for these respective days. This likely contributes a significant amount to the major differences observed in the model comparisons. In addition to this, differences in the fraction of biomass burned, biomass loading
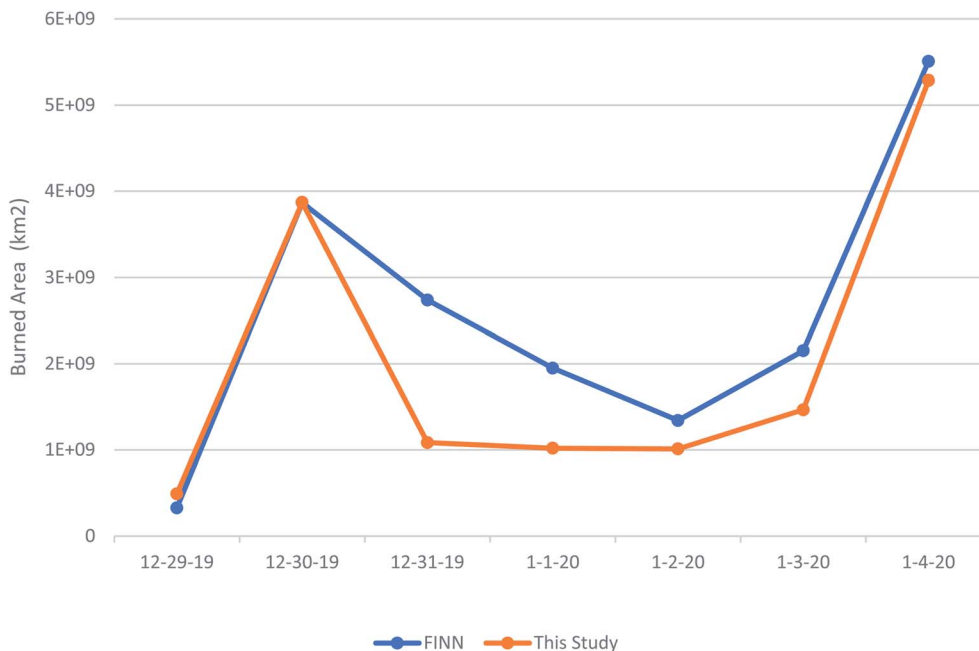
Fig. 4 Comparing burn area estimates from this study with burn area estimates from FINNv2.4.

and emission factors also contributes to the differences in the emissions.

Hourly $PM_{2.5}$ concentrations at the ground measurement sites were examined for December 29, 2019, through January 4, 2020. The hourly $PM_{2.5}$ concentrations at the Australian monitors ranged between 0.1 μg m^{-3} and ~2496 μg m^{-3}, with an average of ~76 μg m^{-3}. At the New Zealand monitors, the hourly $PM_{2.5}$ concentrations were less than ~50 μg m^{-3} with an average of ~8.58 μg m^{-3}. The National Environment Protection Measure for Ambient Air Quality standard for daily $PM_{2.5}$ is 25 μg m^{-3}.[48] During the 2019–2020 wildfires, ground measurement sites measured numerous (greater than 500) exceedance events for $PM_{2.5}$ concentration. Some examples of exceedances in the study region are highlighted below.

Because of their locations, the Australian Capital Territory (ACT) sites are more affected than others. As seen in Fig. 5, the $PM_{2.5}$ standard was exceeded until the 6th of January, with the exceedances of the standard that reached 1500 and 2500 μg m^{-3} on the 1st of January and 5th of January, respectively. Although $PM_{2.5}$ concentration is different in the Monash monitoring site, similar peaks are experienced on the same days, with exceedances that were 80 and 60 times greater than the standard on January 1, 2020, and January 5, 2020, respectively. These peaks can be attributed to both the size and location of the fires as well as meteorological conditions. For example, in the New South Wale (NSW) and Victoria (VIC) regions, temperature anomalies were recorded as +4.31 °C and +3.13 °C, respectively. Accompanying temperature anomalies, low rainfall events likely contributed to a massive number of wildfire events.[30] For the NSW region, exceedance events vary between different locations. According to the Wagga Wagga North monitoring site, peaks are shown on January 2, 2020, and January 5, 2020, with the exceedance on January 5th reaching 72 times higher than the

standard. For the VIC region, fewer standard exceedance events were recorded, which can be attributed to meteorological conditions during the study period. For example, the exceedance on January 3 and 4, 2020, at the Footscray monitoring site only reached ~6 times higher than the standard. Because the Churchill and Moe monitoring sites were not impacted by the wildfire plume, the standard was not exceeded. At three of the New Zealand sites, exceedances that ranged between 1.5 and 2 times the standard were observed on January 1, 2020. These exceedances can be attributed to the transport of pollutants (Fig. 6). However, the Mosgiel and Dunedin monitoring sites were not affected by the concentrated plume.

To understand the contribution these wildfires had on the daily $PM_{2.5}$ concentration, a forward trajectory analysis was performed using the NOAA HYSPLIT model with a 48 h forward trajectory at 500 m for December 29, 2019, through January 4, 2020 using the emissions calculated with the average emission factors, the high-end emission factors and the low-end emission factors. In addition to this, an analysis was also performed using the emissions calculated by FINNv2.4. The results of this model run showed the wildfire emissions transported from the study region in Southeastern Australia to the New Zealand Southwest shore due meteorological conditions (Fig. 6). There was not a significant difference in the modeled trajectories using all four emission inventories. This is unsurprising as the same meteorological data were used in all model runs. The HYSPLIT output provided a range for concentrations of $PM_{2.5}$, which are shown in Fig. 6. The HYSPLIT modeled concentrations of $PM_{2.5}$ using FINNv2.4 were comparable with the modeled concentrations using the inventory created in this work using the average emission factor (Fig. 7). Because FINNv2.4 also uses average emission factors, these results were unsurprising. It was also unsurprising that the modeled
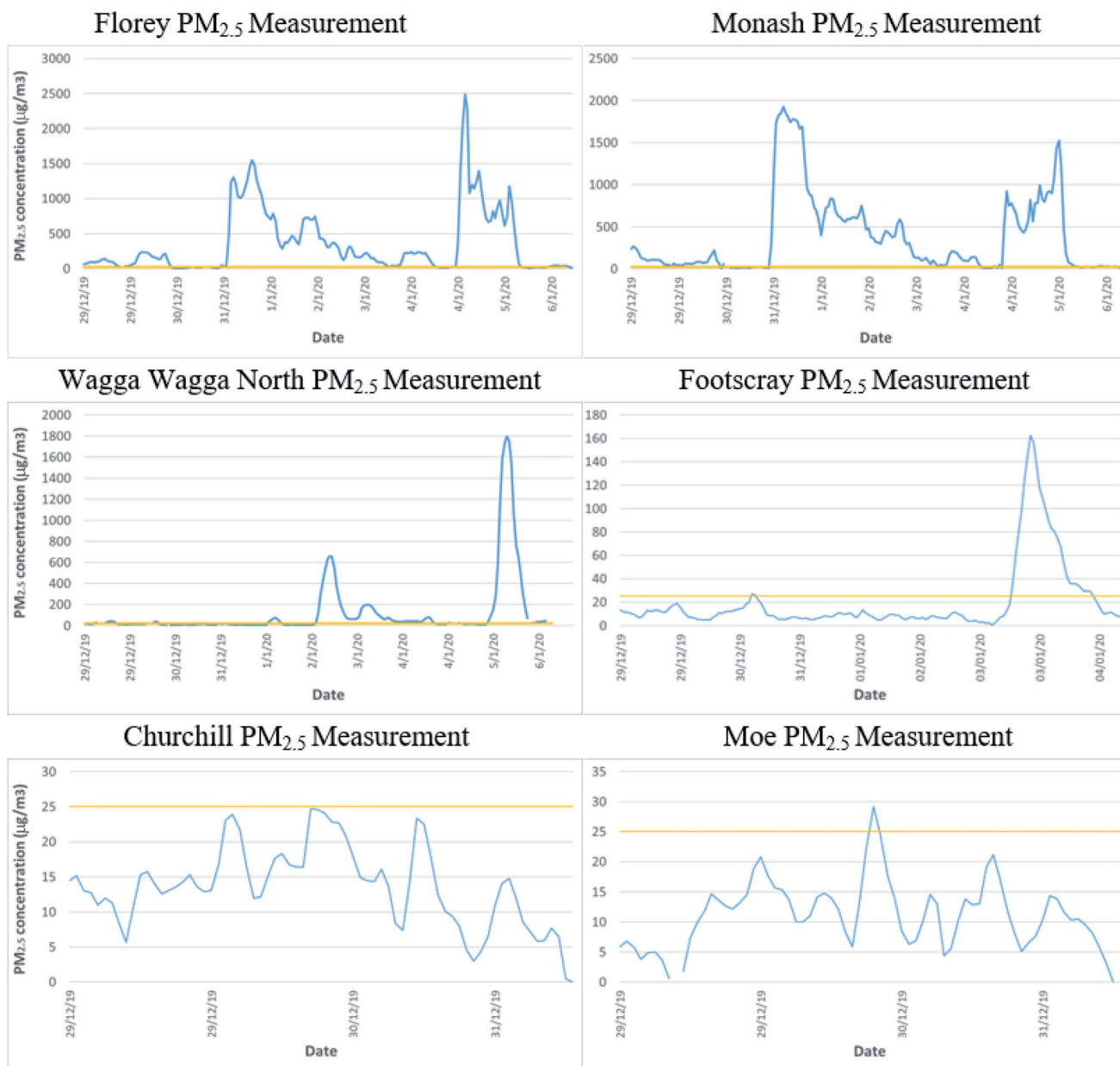
Fig. 5 Hourly PM$_{2.5}$ concentrations (μg m^{-3}) from December 29, 2019, to January 5, 2020, from select monitoring sites. The red line represents the National Environment Protection Measure for Ambient Air Quality national standard for PM$_{2.5}$ (25 μg m^{-3}).

concentrations using FINNv2.4 and the average emission factor inventory were both found to be lower than the modeled concentrations using the high-end emission factor inventory and higher than the concentrations modeled using the low-end emission factor inventory. To compare between modeled and measured PM$_{2.5}$, the concentrations modeled by HYSPLIT were then compared against the ambient concentrations at the measurement sites (Fig. 7). There is a lot of variability when comparing the daily modeled results with the ambient concentrations. For example, the observed concentrations of PM$_{2.5}$ were higher than the all the modeled concentrations from December 29, 2019, and December 31, 2019, and the observed concentrations were similar (~11% higher) to the

concentrations modeled using the high-end emission inventory on December 30, 2019. In contrast to this, the observed concentrations were more comparable to the concentrations modeled using the average emission factor inventory and the low-end emission factor inventory on January 1, 2020, and January 2, 2020, respectively. While the observed concentrations of PM$_{2.5}$ were lower than the concentrations modeled using the high-end emission factor inventory on January 3, 2020, the observed concentrations were higher than the concentrations modeled using FINNv2.4, the average emission factor inventory and the low-end emission factor inventory. In contrast to this, the observed concentrations were only higher than the concentrations modeled using the low-end emission factor
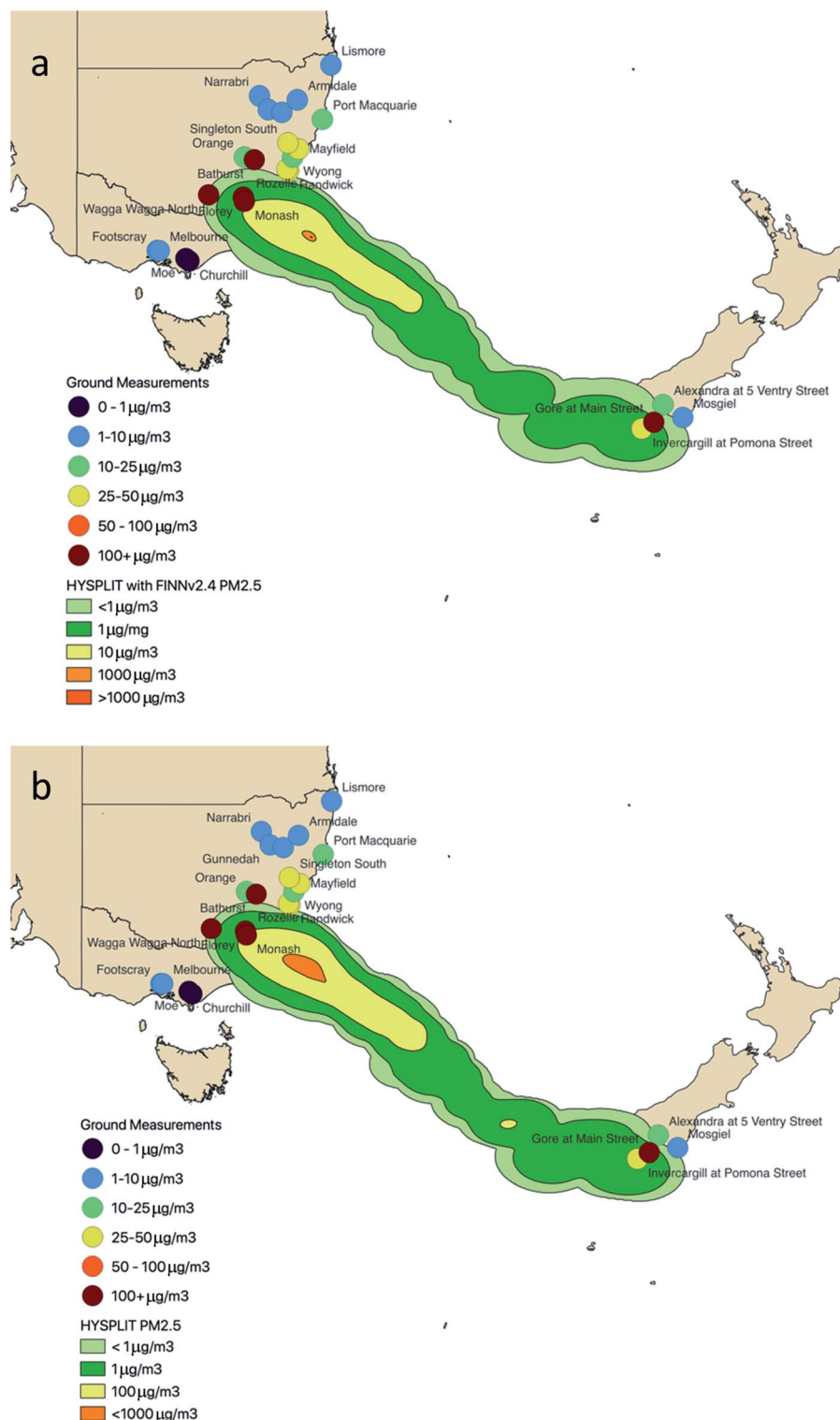
© 2022 The Author(s). Published by the Royal Society of Chemistry

Environ. Sci.: Atmos., 2022, 2, 634–646 | 641

Fig. 6 Distribution and concentration of wildfire plume valid January 1, 2020 0000 UTC plotted with observed ambient concentrations of $PM_{2.5}$. $PM_{2.5}$ distribution and concentration come from only wildfire sources (there are no other external sources).

inventory on January 4–5, 2020, and on January 6, 2020, the modeled concentrations of $PM_{2.5}$ were all higher than the observed concentrations.

Overall, the concentrations modeled using the FINNv2.4 inventory, concentrations ranged from 198% lower to 174%

higher than the observed ambient concentrations. On average, the concentrations modeled using the FINNv2.4 inventory were 70% higher than the observed concentrations. Similarly, when comparing the concentrations modeled using the average emission factor inventory created in this work, the modeled
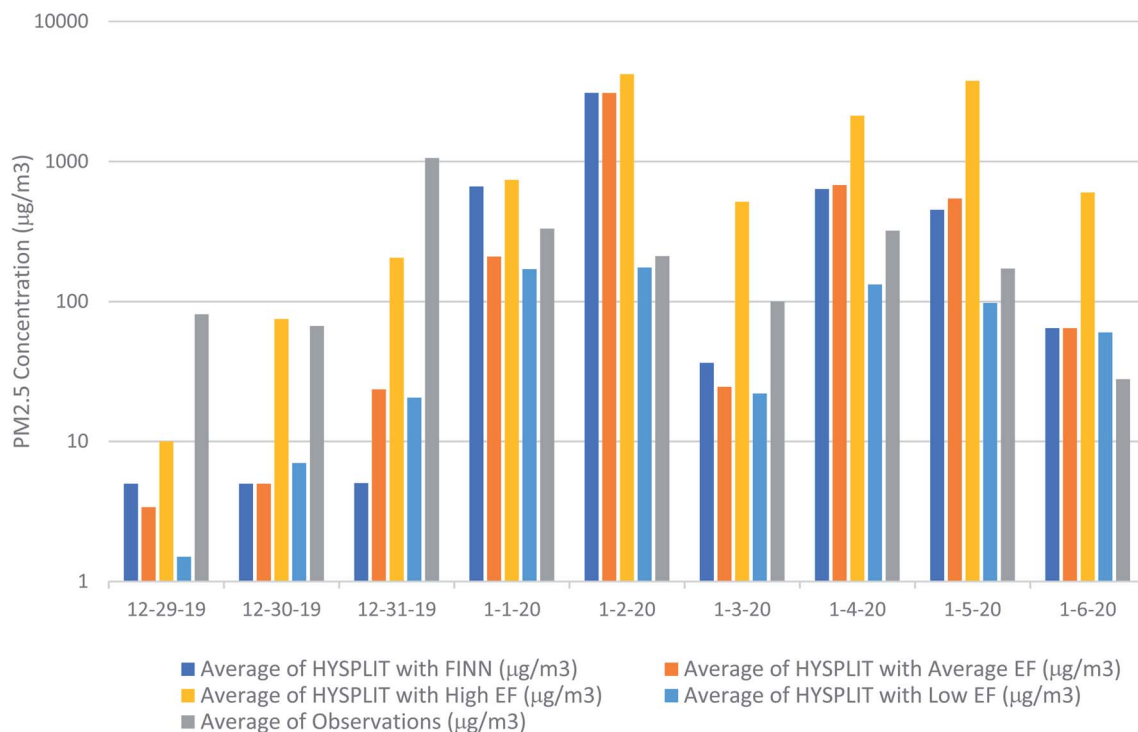
Fig. 7 Comparison of the daily average concentrations of observed $PM_{2.5}$ with the modeled daily average concentrations using emissions calculated by FINN. The comparison includes this work with the average emission factors, the high-end emission factors and the low-end emission factors. Concentrations are plotted on a log scale. It is important to note that the observed concentrations of $PM_{2.5}$ also considers anthropogenic sources therefore it is not an exact comparison.

concentrations ranged from 191% lower to 174% higher than the observed ambient concentrations. On average, concentrations modeled using the emissions created in this work were 65% higher than the observed concentrations. When comparing the concentrations modeled using the high-end emission factor inventory, the modeled concentrations ranged from 156% lower to 182% higher than the observed ambient concentrations and were, on average, 135% higher. In contrast to this, the concentrations modeled using the low-end emission factor inventory, the modeled concentrations ranged from 192% lower to 75% higher than the observed ambient concentrations and were, on average, 110% lower. While all the modeled concentrations vary significantly from the observed concentrations of $PM_{2.5}$, it appears that, on average, the inventories created using the average emission factors yield the most accurate results. The differences between modeled concentrations and the observed concentrations can likely be attributed to the coarseness of the model resolution and the different emission factors used to create the emission inventories. In addition to this, it is important to note that the model does not take other emission sources or atmospheric chemistry into account, therefore secondary $PM_{2.5}$ is not considered in this work.

4. Conclusion

The objective of this study was to estimate emissions of $PM_{2.5}$ and NH_3 from wildfire activity in Southeastern Australia during

peak fire season (December 29, 2019, to January 4, 2020) and then determine the impact that these emissions had on local air quality. Fire activity in the study region consumed 14 230 km^2 of land and produced 526 569 125 kg of NH_3 and 41 167 586 kg of $PM_{2.5}$ during the period of interest. The maximum emissions occurred on January 4, 2020, for both $PM_{2.5}$ (200 481 575 kg) and NH_3 (14 570 058 kg), while minimum emissions occurred on December 29, 2019, for $PM_{2.5}$ (17 338 953 kg) and on January 1, 2020, for NH_3 (919 622 kg).

During large forest fires particles and other gases are injected into atmosphere and transported over long distances affecting air quality in the subsidence regions. Between December 29, 2019, and January 5, 2020, concentrations of $PM_{2.5}$ reached 2496.1 µg m^{-3} in Australia and 48.8 µg m^{-3} in New Zealand, exceeding the national standard of 25 µg m^{-3} a total of 100 and 2 times, respectively. The highest $PM_{2.5}$ concentration exceedances can be attributed to wildfire plume impact. This was observed during the wildfire plume from December 29, 2019, to January 6, 2020. The largest exceedance of the national standard for $PM_{2.5}$ concentration was observed in the ACT region. The highest increase in $PM_{2.5}$ concentration was observed at the Florey monitoring site (~2500 µg m^{-3}). This exceedance was followed at the Monash monitoring site (~2000 µg m^{-3}). In the NSW region, the observed exceedances of the national standard were significantly lower than what was observed in the ACT region, with the exception of the Wagga Wagga North monitoring site, which observed concentrations of ~1800 µg m^{-3}. In contrast to this, the rest of the NSW monitoring sites observed concentrations between

© 2022 The Author(s). Published by the Royal Society of Chemistry

Environ. Sci.: Atmos., 2022, **2**, 634–646 | **643**

$\sim$530 µg m^{-3} and $\sim$75 µg m^{-3}. This can be attributed to the location of the Wagga Wagga North monitoring site, as it is closest to the ACT region while the other monitoring sites are located north of the NSW region. The impact of the wildfire plumes was not as severe in the Victoria region, with the largest exceedance occurring when concentrations of PM$_{2.5}$ reached $\sim$160 µg m^{-3} at the Footscray monitoring site on January 3, 2020. The New Zealand monitoring sites were the least impacted due to the dispersion, diffusion, and deposition the PM$_{2.5}$ in the plume as it was transported. Therefore, the concentration of PM$_{2.5}$ in the plume was diluted by the time it reached New Zealand. The maximum concentration of PM$_{2.5}$ concentration in New Zealand was observed at the Alexandra monitoring site ($\sim$50 µg m^{-3}).

The impact these mega fires had on ambient concentrations was also examined using the NOAA HYSPLIT model. Model runs were conducted for the study period using the inventories created in this work as well as fire emissions quantified by FINNv2.4. There was a lot of variability between the modeled concentrations using each inventory and the observed concentrations of PM$_{2.5}$, with the performance of each inventory varying by day. For example, while the concentrations modeled by the high-emission inventory were the closest to the observed concentrations on December 30, 2019, both FINNv2.4 and the average emission factor inventory created in this work were the closet, on average, to the observed concentrations.

The impact of wildfire on both human health and the environment is significant. As the climate continues to change, increased temperatures and drought will likely lead to longer and more severe fire seasons. Recent fires studies, which aim to prevent intense wildfires now destroying forests across Western North America, suggest that innovative strategies for reducing wild fires may be working by sacrificing some trees to prevent the immolation of all of them. Such management strategies should be considered to mitigate and or reduce wild fires in Australia.

Conflicts of interest

There are no conflicts to declare.

Acknowledgements

References

1 S. Shahparvari, B. Abbasi, P. Chhetri and A. Abareshi, Fleet routing and scheduling in bushfire emergency evacuation: a regional case study of the Black Saturday bushfires in Australia, *Transp. Res. D*, 2019, **67**(February 2009), 703–722, DOI: 10.1016/j.trd.2016.11.015.

2 C. Wilkinson, C. Eriksen and T. Penman, Into the firing line: civilian ingress during the 2013 "Red October" bushfires, Australia, *Nat. Hazards*, 2016, **80**(1), 521–538, DOI: 10.1007/s11069-015-1982-5.

3 H. N. Duc, L. T.-C. Chang, M. Azzi and N. Jiang, Smoke aerosols dispersion and transport from the 2013 New South Wales (Australia) bushfires, *Environ. Monit. Assess.*, 2018, **190**(7), 428, DOI: 10.1007/s10661-018-6810-4.

4 K. Haynes, J. Handmer, J. McAneney, A. Tibbits and L. Coates, Australian bushfire fatalities 1900–2008: exploring trends in relation to the 'prepare, stay and defend or leave early' policy, *Environ. Sci. Policy*, 2010, **13**(3), 185–194. Available from: https://linkinghub.elsevier.com/retrieve/pii/S1462901110000201.

5 S. Shahparvari, B. Abbasi, P. Chhetri and A. Abareshi, Fleet routing and scheduling in bushfire emergency evacuation: a regional case study of the Black Saturday bushfires in Australia, *Transp. Res. D*, 2019, **67**, 703–722. Available from: https://linkinghub.elsevier.com/retrieve/pii/S1361920915301310.

6 F. H. Johnston, Understanding and managing the health impacts of poor air quality from landscape fires, *Med. J. Aust.*, 2017, **207**(6), 229–230, DOI: 10.5694/mja17.00072.

7 H. N. Duc, L. T. C. Chang, M. Azzi and N. Jiang, Smoke aerosols dispersion and transport from the 2013 New South Wales (Australia) bushfires, *Environ. Monit. Assess.*, 2018, **190**(7), 1–22.

8 O. F. Price, G. J. Williamson, S. B. Henderson, F. Johnston and D. M. J. S. Bowman, The Relationship between Particulate Pollution Levels in Australian Cities, Meteorology, and Landscape Fire Activity Detected from MODIS Hotspots, *PLoS One*, 2012, **7**(10), e47327.

9 A. Sapkota, J. M. Symons, J. Kleissl, L. Wang, M. B. Parlange, J. Ondov, et al., Impact of the 2002 Canadian Forest Fires on Particulate Matter Air Quality in Baltimore City, *Environ. Sci. Technol.*, 2005, **39**(1), 24–32, DOI: 10.1021/es035311z.

10 E. K. Wise, Meteorologically influenced wildfire impacts on urban particulate matter and visibility in Tucson, Arizona, USA, *Int. J. Wildland Fire*, 2008, **17**(2), 214. Available from: https://www.publish.csiro.au/?paper=WF06111.

11 C. D. Bray, W. H. Battye and V. P. Aneja, The role of biomass burning agricultural emissions in the Indo-Gangetic Plains on the air quality in New Delhi, India, *Atmos. Environ.*, 2019, **218**, 116983. Available from: https://linkinghub.elsevier.com/retrieve/pii/S1352231019306223.

12 E. Hirsch and I. Koren, Record-breaking aerosol levels explained by smoke injection into the stratosphere, *Atmos. Aerosols*, 2021, 1269–1274.

13 C. Wiedinmyer, B. Quayle, C. Geron, A. Belote, D. McKenzie, X. Zhang, et al., Estimating emissions from fires in North America for air quality modeling, *Atmos. Environ.*, 2006, **40**(19), 3419–3432.

14 C. D. Bray, W. H. Battye, V. P. Aneja and W. H. Schlesinger, Global emissions of NH$_3$, NO$_x$, and N$_2$O from biomass

burning and the impact of climate change, *J. Air Waste Manage. Assoc.*, 2021, **71**(1), 102–114. Available from: **https://www.tandfonline.com/doi/full/10.1080/10962247.2020.1842822**.

15 EPA, *Particulate Matter (PM) Pollution*, 2020, cited 2020 Oct 12. Available from: **https://www.epa.gov/pm-pollution/particulate-matter-pm-basics**.

16 San Joaquin Valley Air Pollution Control District, *Particulate Matter (PM) Sources*, 2020, cited 2020 Oct 12. Available from: **https://www.valleyair.org/air_quality_plans/AQ_plans_PM_sources.htm**.

17 R. Aguilera, T. Corringham, A. Gershunov and T. Benmarhnia, Wildfire smoke impacts respiratory health more than fine particles from other sources: observational evidence from Southern California, *Nat. Commun.*, 2021, **12**(1), 1493. Available from: **https://www.nature.com/articles/s41467-021-21708-0**.

18 EPA, *Visibility and Haze*, 2020, cited 2020 Oct 12. Available from: **https://www.epa.gov/visibility/basic-information-about-visibility**.

19 B. H. Baek, V. P. Aneja and Q. Tong, Chemical coupling between ammonia, acid gases, and fine particles, *Environ. Pollut.*, 2004, **129**(1), 89–98. Available from: **https://linkinghub.elsevier.com/retrieve/pii/S0269749103003816**.

20 B. H. Baek and V. P. Aneja, Measurement and Analysis of the Relationship between Ammonia, Acid Gases, and Fine Particles in Eastern North Carolina, *J. Air Waste Manage. Assoc.*, 2004, **54**(5), 623–633, DOI: **10.1080/10473289.2004.10470933**.

21 S. N. Behera, R. Betha and R. Balasubramanian, Insights into Chemical Coupling among Acidic Gases, Ammonia and Secondary Inorganic Aerosols, *Aerosol Air Qual. Res.*, 2013, **13**(4), 1282–1296. Available from: **https://aaqr.org/articles/aaqr-12-11-oa-0328**.

22 C. D. Bray, W. Battye, V. P. Aneja, D. Q. Tong, P. Lee and Y. Tang, Ammonia emissions from biomass burning in the continental United States, *Atmos. Environ.*, 2018, **187**(December 2017), 50–61, DOI: **10.1016/j.atmosenv.2018.05.052**.

23 X. Chen, D. Day, B. Schichtel, W. Malm, A. K. Matzoll, J. Mojica, *et al.*, Seasonal ambient ammonia and ammonium concentrations in a pilot improve NHx monitoring network in the western United States, *Atmos. Environ.*, 2014, **91**, 118–126. Available from: **https://linkinghub.elsevier.com/retrieve/pii/S135223101400243X**.

24 D. E. Day, X. Chen, K. A. Gebhart, C. M. Carrico, F. M. Schwandner, K. B. Benedict, *et al.*, Spatial and temporal variability of ammonia and other inorganic aerosol species, *Atmos. Environ.*, 2012, **61**, 490–498. Available from: **https://linkinghub.elsevier.com/retrieve/pii/S1352231012006085**.

25 W. Battye, V. P. Aneja and W. H. Schlesinger, Is nitrogen the next carbon?, *Earth's Future*, 2017, **5**(9), 894–904, DOI: **10.1002/2017EF000592**.

26 R. D. Wiegand, *Fine Particulate Matter (PM2.5) Pollution in Intensive Agricultural Region of North Carolina: Satellite Analysis and Integrate Ground-Based Measurements*, North Carolina State University, 2019.

27 A. O. Langford and F. C. Fehsenfeld, Natural Vegetation as a Source or Sink for Atmospheric Ammonia: A Case Study, *Science*, 1992, **255**(5044), 581–583, DOI: **10.1126/science.255.5044.581**.

28 N. J. Abram, B. J. Henley, A. Sen Gupta, T. J. R. Lippmann, H. Clarke, A. J. Dowdy, *et al.*, Connections of climate change and variability to large and extreme forest fires in southeast Australia, *Commun. Earth Environ.*, 2021, **2**(1), 8. Available from: **https://www.nature.com/articles/s43247-020-00065-8**.

29 M. A. Adams, M. Shadmanroodposhti and M. Neumann, Causes and consequences of Eastern Australia's 2019–20 season of mega-fires: a broader perspective, *Glob. Change Biol.*, 2020, **26**(7), 3756–3758, DOI: **10.1111/gcb.15125**.

30 Australian Government Bureau of Meteorology, *Australia in December 2019*, 2020, cited 2021 May 1. Available from: **https://www.bom.gov.au/climate/current/month/aus/archive/201912.summary.shtml**.

31 K. Ohneiser, A. Ansmann, H. Baars, P. Seifert, B. Barja, C. Jimenez, *et al.*, Smoke of extreme Australian bushfires observed in the stratosphere over Punta Arenas, Chile, in January 2020: optical thickness, lidar ratios, and depolarization ratios at 355 and 532 nm, *Atmos. Chem. Phys.*, 2020, **20**(13), 8003–8015. Available from: **https://acp.copernicus.org/articles/20/8003/2020/**.

32 T. Shiraishi and R. Hirata, Estimation of carbon dioxide emissions from the megafires of Australia in 2019–2020, *Sci. Rep.*, 2021, **11**(1), 8267. Available from: **https://www.nature.com/articles/s41598-021-87721-x**.

33 J. Li, Y. Tian, Y. Deng, Y. Zhang and K. Xie, Improving the estimation of greenhouse gas emissions from the Chinese coal-to-electricity chain by a bottom-up approach, *Resour., Conserv. Recycl.*, 2021, **167**, 105237. Available from: **https://linkinghub.elsevier.com/retrieve/pii/S0921344920305528**.

34 A. M. Graham, K. J. Pringle, R. J. Pope, S. R. Arnold, L. A. Conibear, H. Burns, *et al.*, Impact of the 2019/2020 Australian Megafires on Air Quality and Health, *GeoHealth*, 2021, **5**(10), e2021GH000454, DOI: **10.1029/2021GH000454**.

35 A. F. Stein, R. R. Draxler, G. D. Rolph, B. J. B. Stunder, M. D. Cohen and F. Ngan, NOAA's HYSPLIT Atmospheric Transport and Dispersion Modeling System, *Bull. Am. Meteorol. Soc.*, 2015, **96**(12), 2059–2077, DOI: **10.1175/BAMS-D-14-00110.1**.

36 I. Oliveras, L. O. Anderson and Y. Malhi, Application of remote sensing to understanding fire regimes and biomass burning emissions of the tropical Andes, *Global Biogeochem. Cycles*, 2014, **28**(4), 480–496, DOI: **10.1002/2013GB004664**.

37 C. Wiedinmyer, S. K. Akagi, R. J. Yokelson, L. K. Emmons, J. A. Al-Saadi, J. J. Orlando, *et al.*, The Fire INventory from NCAR (FINN): a high resolution global model to estimate the emissions from open burning, *Geosci. Model Dev.*, 2011, **4**(3), 625–641. Available from: **https://gmd.copernicus.org/articles/4/625/2011/**.

38 M. A. Friedl, D. Sulla-Menashe, B. Tan, A. Schneider, N. Ramankutty, A. Sibley, *et al.*, MODIS Collection 5 global land cover: algorithm refinements and characterization of new datasets, *Remote Sens. Environ.*, 2010, **114**(1), 168–182. Available from: **https://linkinghub.elsevier.com/retrieve/pii/S0034425709002673**.

39 M. Friedl and D. Sulla-Menashe, *MCD12Q1 MODIS/Terra+Aqua Land Cover Type Yearly L3 Global 500m SIN Grid V006 [Data set]*, NASA EOSDIS Land Processes DAAC2019, accessed 2022-05-05 from **https://doi.org/10.5067/MODIS/MCD12Q1.006**.

40 A. Ito and J. E. Penner, Global estimates of biomass burning emissions based on satellite imagery for the year 2000, *J. Geophys. Res.*, 2004, **109**(D14), D14S05, DOI: **10.1029/2003JD004423**.

41 University of Washington, *Smoke Emissions Reference Application (SERA)*, 2021.

42 S. K. Akagi, R. J. Yokelson, C. Wiedinmyer, M. J. Alvarado, J. S. Reid, T. Karl, *et al.*, Emission factors for open and domestic biomass burning for use in atmospheric models, *Atmos. Chem. Phys.*, 2011, **11**(9), 4039–4072. Available from: **https://acp.copernicus.org/articles/11/4039/2011/**.

43 M. O. Andreae and P. Metlet, *Emission of Trace Gases and Aerosols from Biomass Burning*, 2001.

44 M. O. Andreae, Emission of trace gases and aerosols from biomass burning – an updated assessment, *Atmos. Chem. Phys.*, 2019, **19**(13), 8523–8546. Available from: **https://acp.copernicus.org/articles/19/8523/2019/**.

45 LAWA, *Air Quality*, 2020. Available from: **https://www.lawa.org.nz/explore-data/air-quality/**.

46 Thermo Fisher Scientific, *FH62C14*, 2010. Available from: **https://assets.thermofisher.com/TFS-Assets/null%7Cnull/Package-Inserts/EPM-manual-FH62C14.pdf**.

47 G. Rolph, A. Stein and B. Stunder, Real-time Environmental Applications and Display sYstem: READY, *Environ. Model. Softw.*, 2017, **95**, 210–228, DOI: **10.1016/j.envsoft.2017.06.025**.

48 Australia State of the Environment, *National Air Quality Standards: Ambient Air Quality*, 2016, cited 2021 May 1. Available from: **https://soe.environment.gov.au/theme/ambient-air-quality/topic/2016/national-air-quality-standards**.